

REPUBLIC OF AZERBAIJAN

On the rights of the manuscript

ABSTRACT

of the dissertation for the degree of Doctor of Philosophy

**LOCAL STRUCTURE AND PHYSICAL PROPERTIES OF
THE GeAsSeS GLASSY SYSTEM IN ELASTIC, ISOSTATIC,
AND STRESSED-RIGID PHASES**

Speciality: 2220.01- Semiconductor Physics

Field of Science: Physics

Applicant: **Samir Mehman Mammadov**

Baku-2025

The work was performed at Institute of Physics of the Ministry of Science and Education Republic of Azerbaijan laboratory of “Physics and electronics of non-crystalline semiconductors”.

Scientific Supervisors: Corresponding member of ANAS,
Doctor of Science in Physics and
Mathematics, Professor
Salima Ibrahim Mehdiyeva

Doctor of Science in Physics,
Associate Professor
Rahim Ibad Alekberov

Official Opponents: Doctor of Sciences in Physics and
Mathematics, Professor
Zakir Agasoltan Cahangirli

Doctor of Sciences in Physics and
Mathematics, Professor
Kerim Rehim Allahverdiyev

Doctor of Sciences in Physics and
Mathematics, Professor
Maarif Ali Jafarov

Dissertation council ED 1.14 of Supreme Attestation Commission under the President of the Republic of Azerbaijan operating at Institute of Physics of Ministry of Science and Education Republic of Azerbaijan

Chairman of the

Dissertation Council: Academician
Arif Mammad Hashimov

Scientific Secretary of the
Dissertation Council: Doctor of Science in Physics, Professor
Rafiga Zabil Mehdiyeva

Chairman of the
Scientific Seminar: Doctor of Sciences in Physics and
Mathematics, Professor
Huseyn Behbud Ibragimov



GENERAL DESCRIPTION OF WORK

The actuality of the subject and degree of elaboration:

For the lossless transmission of optical signals, the development of fiber-optic materials with advanced technological characteristics and optimal parameters, as well as their successful application, is regarded as one of the major challenges of the modern optoelectronic industry. In this regard, there is an urgent need for the synthesis of new functional materials whose compositions, in addition to being resistant to crystallization, also exhibit high values of thermal stability, chemical durability, and glass-forming ability, as well as for the investigation of their physical properties. Taking this into account, studying the reasons for the high values of these parameters in the investigated substances, and linking them to their local structure, the nature of their thermal and optical properties, and their underlying physical mechanisms, is of both scientific and practical significance.

Scientific studies demonstrate that the presence of structural and thermal instabilities in simple and binary chalcogenide glasses imposes limitations on their application in fibers. Therefore, the synthesis of materials with the required glass transition temperature (T_g) and thermal expansion coefficient, and the investigation of their thermal and optical properties, is particularly essential for fiber optics¹. In this regard, preparation of multicomponent chalcogenide glassy materials with wide functional capabilities, along with the study of their physical properties, provides a favorable basis for practical applications.

The scientific investigations presented in this dissertation demonstrate that, within the Ge-As-Se-S chalcogenide glassy system, it is possible to obtain materials with high glass-forming ability (Hruby number, Hr), enhanced thermal stability parameters (H^1 , S), and widely tunable optical properties by deliberately varying the atomic percent ratios of chalcogen (Se, S) and non-chalcogen (Ge, As) components. Consequently, the precise investigation of the mechanisms governing

¹ Zahng Y. Raman gain and femtosecond laser induced damage of Ge-As-S chalcogenide glasses / Yan Zhang, Yinsheng Xu, Chenyang You [et al.] // Opt Express, -2017; ;25(8): -p.8886-8895

the relationships between local structure and physical properties in various topological glass states (elastic, isostatic, and stressed-rigid) is both scientifically and practically relevant.

The object and subject of the research:

The object of the research is represented by the $\text{Ge}_4\text{As}_{14}\text{Se}_{82}$, $\text{Ge}_4\text{As}_{14}\text{Se}_{80}\text{S}_2$, $\text{Ge}_7\text{As}_{16}\text{Se}_{72}\text{S}_5$, $\text{Ge}_{10}\text{As}_{20}\text{Se}_{60}\text{S}_{10}$, $\text{Ge}_{17.5}\text{As}_{15}\text{Se}_{52.5}\text{S}_{15}$, $\text{Ge}_{24}\text{As}_{19}\text{Se}_{37}\text{S}_{20}$, $\text{Ge}_{25}\text{As}_{10}\text{Se}_{40}\text{S}_{25}$, $\text{Ge}_{26}\text{As}_{18}\text{Se}_{26}\text{S}_{30}$, and $\text{Ge}_{33}\text{As}_{17}\text{Se}_{15}\text{S}_{35}$ systems, synthesized on the basis of germanium and arsenic (Ge, As) chalcogenides; the subject of the research is the investigation of the local structure and physical properties of these materials in the elastic, isostatic, and stressed-rigid regions.

The purpose and tasks of the research

The aim of the research is to determine the mechanisms by which chalcogen (Se, S) and non-chalcogen (Ge, As) modifiers influence various topological glass states (elastic, isostatic, and stressed-rigid), their local structure, glass-forming ability, thermal stability, glass and crystallization domains, and optical parameters within the Ge-As-Se-S glassy systems.

The practical objective of the work is the synthesis of new functional materials with high crystallization resistance, thermal stability, and glass-forming ability (H_r) for use in passive fiber transmitters.

- Multicomponent Ge-As-Se-S compounds with various topological glass states (isostatic, stressed-rigid, and elastic), namely $\text{Ge}_4\text{As}_{14}\text{Se}_{82}$, $\text{Ge}_4\text{As}_{14}\text{Se}_{80}\text{S}_2$, $\text{Ge}_7\text{As}_{16}\text{Se}_{72}\text{S}_5$, $\text{Ge}_{10}\text{As}_{20}\text{Se}_{60}\text{S}_{10}$, $\text{Ge}_{17.5}\text{As}_{15}\text{Se}_{52.5}\text{S}_{15}$, $\text{Ge}_{24}\text{As}_{19}\text{Se}_{37}\text{S}_{20}$, $\text{Ge}_{25}\text{As}_{10}\text{Se}_{40}\text{S}_{25}$, $\text{Ge}_{26}\text{As}_{18}\text{Se}_{26}\text{S}_{30}$, and $\text{Ge}_{33}\text{As}_{17}\text{Se}_{15}\text{S}_{35}$, have been synthesized;

- The local structure of the synthesized materials has been examined using X-ray diffraction scattering, while their composition has been determined by energy-dispersive X-ray analysis;

- Various bonds and structural units (pyramidal and tetrahedral) constituting the local structure of the synthesized materials have been identified through Raman spectroscopy;

- The glass and crystallization processes, glass-forming ability, crystallization rate parameters, and their correlation with local structural parameters have been investigated by differential scanning

calorimetry, within the framework of topological constraint theory, the layered structure concept, and the chemically ordered network model;

- The optical absorption of thin films obtained by thermal evaporation in vacuum has been studied, taking into account the fractal characteristics of the material;

- The effect of hydrocarbon environments on the current–voltage characteristics (I–V curves) of sandwich-structured thin films prepared by thermal evaporation in vacuum, as well as their application-related properties, has been investigated.

Research methods:

In the study of the local structure, glass and crystallization processes, glass-forming ability, thermal stability, and optical parameters of the Ge-As-Se-S glassy systems in various topological glass states, X-ray diffraction, differential scanning calorimetry, Raman spectroscopy, and optical spectroscopy methods have been employed.

The main provisions submitted to the defense:

1. A decrease in the crystallization exponent (n), which characterizes the temperature dependence of the crystalline volume fraction, and a reduction in the index crystallation rapidity (ICR) due to the joint increase in the relative concentration of tetrahedral ($\text{GeS}_{4/2}$, $\text{GeSe}_{4/2}$) and pyramidal ($\text{AsSe}_{3/2}$) structural units forming the amorphous matrix of the Ge-As-Se-S chalcogenide glassy system;

2. Identification of correlational relationships between the decrease in the index crystallation rapidity (ICR) and the increase in the bond connectivity of the amorphous matrix, including the growth of the mean bond energy ($\langle E \rangle$);

3. In materials close to the topological ordering condition ($f \sim 0$; $N_{co} \sim 3$), the index crystallation rapidity (ICR) is low, while the difference between the glass transition and crystallization temperatures ($\Delta T_{c-g} = 71\text{--}87\text{ K}$) is relatively high;

4. In the composition $\text{Ge}_{33}\text{As}_{17}\text{Se}_{15}\text{S}_{35}$, which has a high atomic fraction of germanium, the crystallization process is accelerated, accompanied by a significant decrease in the numerical value of the temperature difference between glass transition and crystallization ($\Delta T_{c-g} = 60\text{ K}$);

5. The results obtained from the spectral dependences of the

optical absorption coefficient in the exponential region have been associated with the fractal nature of the material.

Scientific novelty of the study:

● In the Ge-As-Se-S chalcogenide glassy systems, the crystallization exponent (n) in the exponential region of optical absorption assumes various values differing from $n = 1.5$ and 2 . This deviation, along with the departure of the density of states versus energy dependence from that of free-electron states, is attributed to the fractal nature of the material;

● It has been demonstrated that samples close to the topological ($f \sim 0$) and chemical ordering ($R=1$) conditions, and resistant to crystallization ($\Delta T_{c-g} \sim 87$ K), possess promising potential for application in passive fiber optics;

● It has been shown that the primary structural units forming the amorphous matrix ($AsSe_{3/2}$, $GeS_{4/2}$, $GeSe_{4/2}$) have a significant effect on the index crystallation rapidity (ICR) and the temperature difference between glass transition and crystallization (ΔT_{c-g});

● In the composition $Ge_{33}As_{17}Se_{15}S_{35}$, which has a high germanium content, the acceleration of the crystallization process and the sharp decrease in the glass transition–crystallization temperature difference (ΔT_{c-g}) are associated with weak local structural transformations;

● For the compositions $Ge_{17.5}As_{15}Se_{52.5}S_{15}$, $Ge_{24}As_{19}Se_{37}S_{20}$, $Ge_{25}As_{10}Se_{40}S_{25}$, $Ge_{26}As_{18}Se_{26}S_{30}$ corresponding to an average coordination number $Z = 2.5-2.7$, the Porod exponent (n_P) varies within the interval $1 < n_P < 3$, which is related to the transformation of rough-surfaced scattering centers into spatial (three-dimensional) fractals;

● Under the influence of a hydrocarbon environment, current oscillations in the current–voltage characteristics of Al- $Ge_{33}As_{17}Se_{15}S_{35}$ -Te sandwich structures are weakened and eventually suppressed.

Theoretical and practical significance of the study:

The results of the dissertation can be applied to the investigation of glass and crystallization processes in multicomponent glassy materials based on germanium and arsenic (Ge, As) chalcogenides in elastic, isostatic, and stressed-rigid states, as well as to the study of their

mechanisms of influence on optical absorption.

Multicomponent and crystallization-resistant samples such as $\text{Ge}_4\text{As}_{14}\text{Se}_{82}$, $\text{Ge}_4\text{As}_{14}\text{Se}_{80}\text{S}_2$, $\text{Ge}_7\text{As}_{16}\text{Se}_{72}\text{S}_5$, $\text{Ge}_{10}\text{As}_{20}\text{Se}_{60}\text{S}_{10}$, $\text{Ge}_{17.5}\text{As}_{15}\text{Se}_{52.5}\text{S}_{15}$, $\text{Ge}_{24}\text{As}_{19}\text{Se}_{37}\text{S}_{20}$, $\text{Ge}_{25}\text{As}_{10}\text{Se}_{40}\text{S}_{25}$, $\text{Ge}_{26}\text{As}_{18}\text{Se}_{26}\text{S}_{30}$ and $\text{Ge}_{33}\text{As}_{17}\text{Se}_{15}\text{S}_{35}$ may be successfully employed in passive fiber optics and gas sensors.

Approbation and application:

The results of the dissertation were presented at the following scientific conferences:

- Akademik L.M. İmanovun 100 illik yubileyinə həsr olunmuş Molekulyar spektroskopiya mövzusunda konfrans, Azərbaycan və rus dillərində məqalələr (Bakı-Şuşa, 2022);

- H. Əliyevin 100 illiyinə həsr olunmuş nəzəri və tətbiqi fizikanın inkişafı mövzusunda beynəlxalq konfrans (Bakı, 2023);

- Конференция; Аморфные и микрокристаллические полупроводники (Санкт-Петербург, Россия, 2023);

- International Conference on Advanced Laser Technologies (ALT) (LS-I-10, Samara, Russia, 2023);

- Müasir təbiət və iqtisad elmlərinin aktual problemləri Beynəlxalq Elmi Konfrans (Gəncə, 2023);

- Fizikanın aktual problemləri mövzusunda Beynəlxalq Elmi Konfrans (Naxçıvan, 2024);

- The 31th International Conference on Advanced Laser Technologies (ALT) (Vladivostok, Russia, 2024);

15 scientific works have been published in local and foreign scientific publications on the subject of the dissertation work. 8 of them are articles and 7 are conference materials.

Name of the organization where the dissertation work is done:

The dissertation work was performed at the Institute of Physics of the Ministry of Science and Education of the Republic of Azerbaijan.

The structure and volume of the dissertation:

The dissertation is presented in 144 pages, consisting of an introduction, four chapters, conclusions and a bibliographic list of 158 cited literature. There are 26 pictures and 14 tables in the dissertation

work. The total volume of the dissertation consists of 171950 characters.

THE MAIN CONTENT OF THE DISSERTATION

In the introduction, the relevance of the dissertation topic has been substantiated, the objectives of the study, its scientific novelty, and practical significance have been outlined, the main scientific provisions submitted for defense, the degree of approbation, and publications have been presented, and the main content of the chapters has been briefly summarized.

The first chapter provides a review of contemporary research on the atomic and local structure of amorphous and glassy materials, as well as on the investigation of their physical parameters. These materials are non-crystalline solids with a disordered atomic structure. Chalcogenide glasses, being part of the group of amorphous materials, exist not in thermodynamic equilibrium but in a quasi-equilibrium state. Such a non-crystalline structure significantly affects the physical properties of amorphous glasses, including optical, electronic, thermal, and mechanical parameters.

In chalcogenide glassy semiconductors, it is not the long-range order but the short- and medium-range order that plays the key role in determining their properties. Short-range order refers to the arrangement of atoms within a few atomic distances (generally 2–5 Å), which is crucial for understanding the local structural features of amorphous materials. Medium-range order corresponds to a distance range of approximately 5–20 Å and significantly influences the physical properties of the materials.

Like other semiconductor materials, amorphous chalcogenides are characterized both by their structural features and by the width of their forbidden energy gap. Chalcogenide glassy semiconductors are primarily composed of Group VI elements—sulfur, selenium, tellurium—and their compounds with elements such as Ge, As, and Sb.

Chalcogenide glasses containing three- and four-coordinated elements (arsenic, antimony, silicon, germanium), particularly Ge–As–Se–S systems, are of great interest in this regard, as their optical

transparency, band gap width, hardness, and thermal stability can be varied over a wide range.

Due to structural disorder in chalcogenide glasses, bond lengths and bond angles vary, while covalent bonding predominates. Chalcogen atoms possess lone-pair electron configurations, which fundamentally affect optical transitions in these materials. Amorphous structures are mainly composed of heteropolar bonds (Ge–S, As–Se) and, in some cases, homopolar bonds (Se–Se)².

In Ge–Se chalcogenide glasses, Se atoms form chain-like structural units throughout the glass network. The addition of germanium leads to tetrahedral structures centered on Ge and pyramidal structures centered on As, which influence the brittleness and optical properties of the glass.

The local structure, glass and crystallization processes, and optical properties of simple, binary, and more complex chalcogenide glasses have been extensively analyzed. The analysis demonstrates that for multicomponent glassy materials based on germanium and arsenic (Ge, As) chalcogenides, there is a critical need to study the glass formation and crystallization processes, as well as their mechanisms affecting optical absorption, in elastic, isostatic, and stressed-rigid states using various theoretical models and approaches.

Chapter Two is devoted to the synthesis of amorphous and glassy materials and provides a detailed account of the synthesis procedures applied to the selected compositions Ge₄As₁₄Se₈₂, Ge₄As₁₄Se₈₀S₂, Ge₇As₁₆Se₇₂S₅, Ge₁₀As₂₀Se₆₀S₁₀, Ge_{17.5}As₁₅Se_{52.5}S₁₅, Ge₂₄As₁₉Se₃₇S₂₀, Ge₂₅As₁₀Se₄₀S₂₅, Ge₂₆As₁₈Se₂₆S₃₀, Ge₃₃As₁₇Se₁₅S₃₅, which served as the main objects of this study. In addition, the chapter outlines the experimental techniques employed for structural characterization and compositional analysis of these systems.

For all investigated samples, the EDS results were obtained with an accuracy in the range of ± 0.04 – 0.20 (Fig. 1),.

A central objective of this research was to reveal the correlation between the local structural features of the synthesized compositions

² Shi, K. Sulfur chains glass formed by fast compression; Shi, K., Dong, X., Zhao, Z. et al. // Nat Commun 16, 2025, 357.

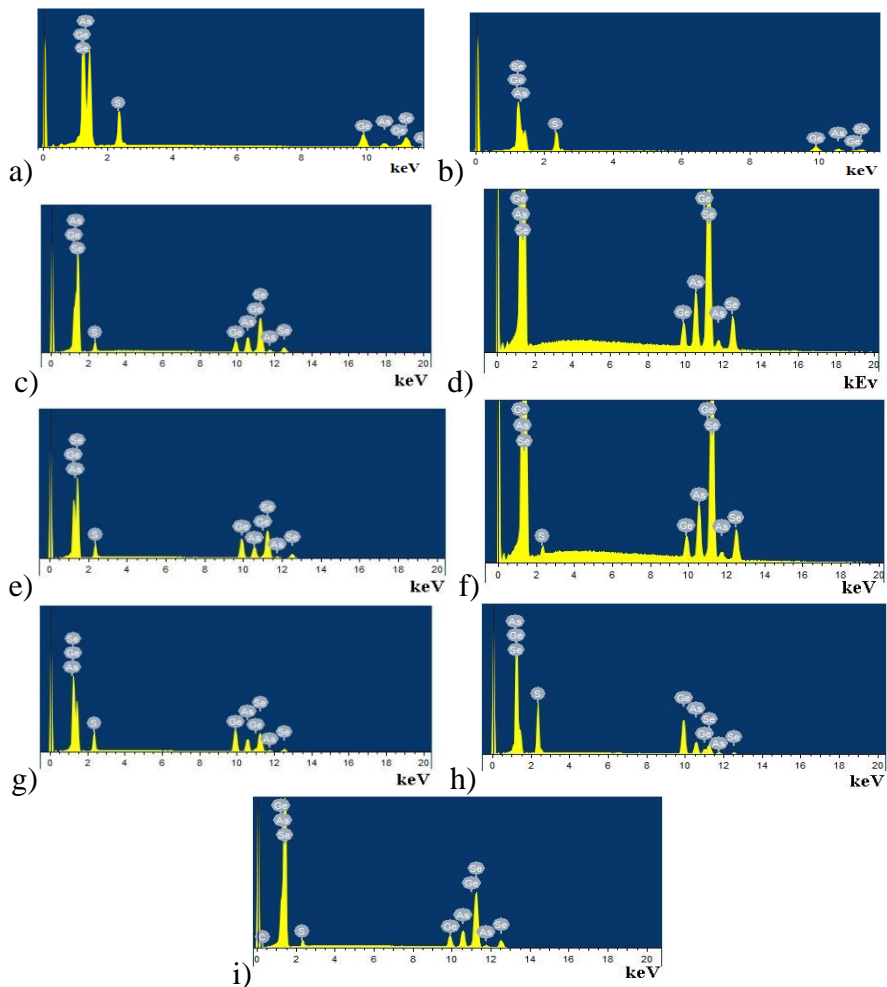


Fig.1. EDS analysis of $\text{Ge}_{25.10}\text{As}_{9.86}\text{Se}_{40.19}\text{S}_{24.85}$ (a), $\text{Ge}_{26.09}\text{As}_{18.05}\text{Se}_{25.96}\text{S}_{29.90}$ (b), $\text{Ge}_{10.41}\text{As}_{20.95}\text{Se}_{59.42}\text{S}_{9.22}$ (c), $\text{Ge}_{19.52}\text{As}_{16.16}\text{Se}_{51.56}\text{S}_{12.76}$ (d), $\text{Ge}_{24.76}\text{As}_{19.68}\text{Se}_{37.06}\text{S}_{18.51}$ (e), $\text{Ge}_{35.16}\text{As}_{14.84}\text{Se}_{15.66}\text{S}_{34.34}$ (f), $\text{Ge}_{4.17}\text{As}_{15.05}\text{Se}_{80.78}$ (g), $\text{Ge}_{3.68}\text{As}_{15.19}\text{Se}_{79.44}\text{S}_{1.69}$ (h), $\text{Ge}_{33}\text{As}_{17.00}\text{Se}_{71.64}\text{S}_{4.03}$ (i).

and their glass transition temperatures (T_g). The local structure of the synthesized samples was studied using a D2 Phaser powder diffractometer (Fig. 2), and the diffraction curves were analyzed with specialized software. The peak amplitude, position, and the full width at half maximum (ΔQ) were determined (FWHM). The amorphous nature of the studied chalcogenide glasses was confirmed by the presence of broad halos in their X-ray diffraction patterns. As illustrated in Fig. 2, all samples exhibit a characteristic first sharp diffraction peak (FSDP) within the scattering vector range $Q = 0.99\text{--}1.41 \text{ \AA}^{-1}$, which reflects medium-range structural ordering typical of amorphous chalcogenide systems.

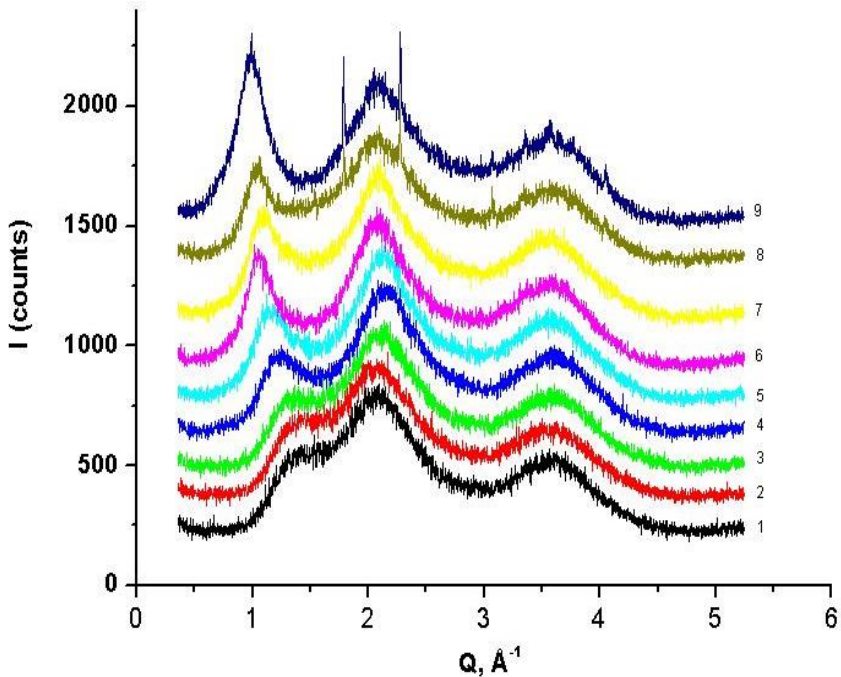


Fig.2. X-ray diffraction patterns: 1- $\text{Ge}_4\text{As}_{14}\text{Se}_{82}$, 2- $\text{Ge}_4\text{As}_{14}\text{Se}_{80}\text{S}_2$, 3- $\text{Ge}_7\text{As}_{16}\text{Se}_{72}\text{S}_5$, 4- $\text{Ge}_{10}\text{As}_{20}\text{Se}_{60}\text{S}_{10}$, 5- $\text{Ge}_{17.5}\text{As}_{15}\text{Se}_{52.5}\text{S}_{15}$, 6- $\text{Ge}_{24}\text{As}_{19}\text{Se}_{37}\text{S}_{20}$, 7- $\text{Ge}_{25}\text{As}_{10}\text{Se}_{40}\text{S}_{25}$, 8- $\text{Ge}_{26}\text{As}_{18}\text{Se}_{26}\text{S}_{30}$, 9- $\text{Ge}_{33}\text{As}_{17}\text{Se}_{15}\text{S}_{35}$

Table 1
Value of Z, R, Q1, N, f and $\Delta Q1$ of synthesis materials

Composition	Z	R	Q1	$L=2\pi/\Delta Q1$	$N_{co}=Z/2+2Z^{-2}$	$N_e=Z/2$	$N_{\beta}=2Z-3$	$f=(12-5Z)/6$	$\Delta Q1$
Ge ₄ As ₁₄ Se ₈₂	2,22	2,83	1,41	22,28	2,55	1,11	1,44	0,15	0,28191
Ge ₄ As ₁₄ Se ₈₀ S ₂	2,22	2,83	1,40	23,4098	2,55	1,11	1,44	0,15	0,26848
Ge ₇ As ₁₆ Se ₇₂ S ₅	2,30	2,03	1,37	22,9649	2,75	1,15	1,60	0,08	0,27359
Ge ₁₀ As ₂₀ Se ₆₀ S ₁₀	2,40	1,40	1,25	24,2631	3,00	1,20	1,80	0,00	0,25896
Ge _{17,5} As ₁₅ Se _{52,5} S ₁₅	2,50	1,17	1,12	25,3764	3,25	1,25	2,00	-0,08	0,24762
Ge ₂₄ As ₁₉ Se ₃₇ S ₂₀	2,67	0,75	1,02	31,3845	3,68	1,34	2,34	-0,23	0,20020
Ge ₂₅ As ₁₀ Se ₄₀ S ₂₅	2,60	1,00	1,10	26,5966	3,50	1,30	2,20	-0,17	0,23624
Ge ₂₆ As ₁₈ Se ₂₆ S ₃₀	2,70	0,71	1,06	27,8473	3,75	1,35	2,40	-0,25	0,22563
Ge ₃₃ As ₁₇ Se ₁₅ S ₃₅	2,83	0,55	0,99	33,7461	4,08	1,42	2,66	-0,36	0,18619

The first sharp diffraction peak (FSDP) is associated with the presence of medium-range order in covalently bonded amorphous materials. For the studied multicomponent chalcogenide glasses, the mean coordination number (Z) and the ratio of the number of covalently bonded chalcogen atoms to that of non-chalcogen atoms (R) were calculated and are presented in Table 1. Based on the application of the topological constraint theory (TCT)³, it follows that for the Ge₁₀As₂₀S₁₀Se₆₀ composition, the mean coordination number satisfies the condition $Z = 2.4$. Consequently, the fraction of zero-frequency vibrational modes in the chalcogenide glassy network becomes $f = 0$, which, according to the theory, corresponds to the “isostatic glass” state.

When $Z < 2.4$, the decrease in the concentrations of germanium, arsenic, and sulfur, accompanied by an increase in selenium content, leads to a corresponding increase in the value of f-

³ J.C. Phillips, Constraint Theory, Vector Percolation and Glass Formation // Solid State Communications/ 1985, 53(8), pp. 699–702.

parametre, satisfying the condition $f > 0$.

As a result, the number of bond-stretching and bond-bending constraints (N_α and N_β) within the glassy network decreases, leading to a total number of constraints lower than three ($N_{co} < 3$). This condition corresponds to the formation of the "floppy glass" state, where the number of degrees of freedom is equal to three. According to the established theory, compositions that satisfy the condition $N_{co} < 3$ ($\text{Ge}_4\text{As}_{14}\text{Se}_{82}$, $\text{Ge}_4\text{As}_{14}\text{Se}_{80}\text{S}_2$, $\text{Ge}_7\text{As}_{16}\text{Se}_{72}\text{S}_5$) should exhibit a higher tendency toward crystallization. Indeed, the results of X-ray diffraction scattering confirm that the medium-range order in these compositions is partially reduced. Thus, the experimental findings are in agreement with the predictions of the topological constraint theory (TCT).

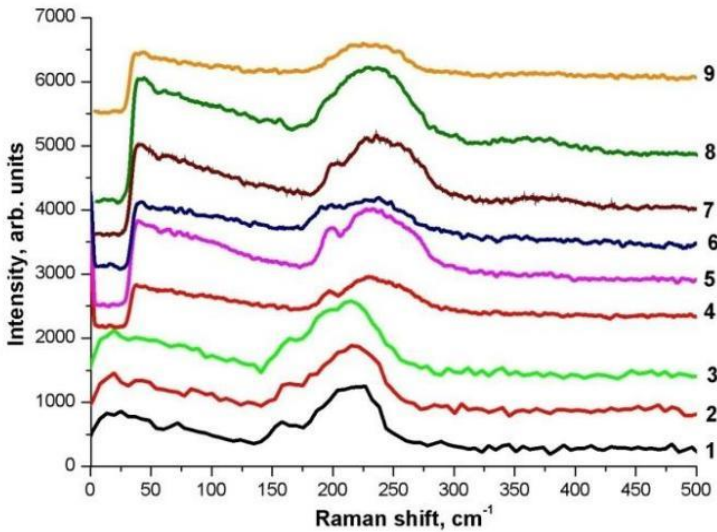


Fig.3. Raman shift: 1 - $\text{Ge}_4\text{As}_{14}\text{Se}_{82}$, 2 - $\text{Ge}_4\text{As}_{14}\text{Se}_{80}\text{S}_2$, 3 - $\text{Ge}_7\text{As}_{16}\text{Se}_{72}\text{S}_5$, 4 - $\text{Ge}_{10}\text{As}_{20}\text{Se}_{60}\text{S}_{10}$, 5 - $\text{Ge}_{17,5}\text{As}_{15}\text{Se}_{52,5}\text{S}_{15}$, 6 - $\text{Ge}_{24}\text{As}_{19}\text{Se}_{37}\text{S}_{20}$, 7 - $\text{Ge}_{25}\text{As}_{10}\text{Se}_{40}\text{S}_{25}$, 8 - $\text{Ge}_{26}\text{As}_{18}\text{Se}_{26}\text{S}_{30}$, 9 - $\text{Ge}_{33}\text{As}_{17}\text{Se}_{15}\text{S}_{35}$

According to TCT, when the mean coordination number exceeds the threshold value ($Z > 2.4$) and the number of constraints satisfies the condition $N_{co} > 3$, the material transitions into a "stressed-rigid glass" state. In this case, the glassy network becomes unstable: weak angular and bond-stretching constraints give rise to stronger internal compressive and tensile stresses. The theory predicts that increasing internal stresses enhance the tendency of the system toward crystallization.

It was established that for compositions corresponding to the stressed-rigid glass state ($Z = 2.5$ ($\text{Ge}_{17.5}\text{As}_{15}\text{Se}_{52.5}\text{S}_{15}$), $Z = 2.67$ ($\text{Ge}_{24}\text{As}_{19}\text{Se}_{37}\text{S}_{20}$), $Z = 2.6$ ($\text{Ge}_{25}\text{As}_{10}\text{Se}_{40}\text{S}_{25}$), $Z = 2.70$ ($\text{Ge}_{26}\text{As}_{18}\text{Se}_{26}\text{S}_{30}$), $Z = 2.83$ ($\text{Ge}_{33}\text{As}_{17}\text{Se}_{15}\text{S}_{35}$)), the size of medium-range order increases comparatively.

Raman spectroscopic studies were carried out on thin films with a thickness of $d = 2 \mu\text{m}$ within the frequency range of $\nu = 25\text{--}500 \text{ cm}^{-1}$ (Fig. 3). The first low-frequency scattering band observed in the spectra is primarily associated with the presence of the first sharp diffraction peak (FSDP), which is characteristic of chalcogenide glasses⁴.

For compositions with a high germanium concentration, namely $\text{Ge}_{26}\text{As}_{18}\text{S}_{30}\text{Se}_{26}$ and $\text{Ge}_{33}\text{As}_{17}\text{S}_{35}\text{Se}_{15}$, the frequency range $\nu = 180\text{--}203 \text{ cm}^{-1}$ corresponds to the vibrational modes of corner-sharing $\text{GeSe}_{4/2}$ tetrahedra. Broad peaks observed in the $\nu = 210\text{--}215 \text{ cm}^{-1}$ range are primarily associated with the vibrational modes of edge-sharing $\text{GeSe}_{4/2}$ tetrahedra. In compositions with a higher arsenic concentration, peaks appear in the $\nu = 215\text{--}226 \text{ cm}^{-1}$ range, which are attributed to the vibrational modes of $\text{AsSe}_{3/2}$ pyramidal structural units.

This chapter also presents the results of optical spectroscopy investigations. These measurements were performed at room temperature using a SPEKOL 1500 UV-VIS spectrophotometer over the wavelength range $\lambda = 190\text{--}1100 \text{ nm}$. Sample-specific optical

⁴ Rongping Wang, Structural and physical properties of $\text{Ge}_{11.5}\text{As}_{24}\text{S}_{64.5-x}\text{Se}_{64.5-(1-x)}$ glasses / Rongping Wang, Kunlun Yan, Zhiyong Yang, Barry Luther-Davies.// Journal of Non-Crystalline Solids 427, -2015, 16–19

parameters were calculated using the software provided with the instrument. The photometric accuracy of the spectrophotometer was approximately 0.01 Å.

The reason amorphous semiconductors exhibit distinct optical properties lies in the presence of a nonzero density of states within the mobility gap. This arises from the absence of sharp band edges, characteristic of crystalline materials, and the presence of localized or additional states near these edges. Localized states are primarily formed due to structural disorder. At present, no theory provides a perfect description of the energy distribution of the density of states, which calls for further detailed experimental investigations. It has been established that the exponent m in the Tauc relation varies within the range $m=1.8-2.2$. At temperatures above the glass transition temperature (T_g), thermal treatment leads to an increase in the exponent m of the Tauc dependence, accompanied by a decrease in the optical band gap (E_g). This behavior is explained by the rise in the concentration of localized states near the conduction and valence band edges as a result of bond breaking during thermal processing at temperatures higher than T_g ⁵.

Transitions from tail states in the valence band to extended states in the conduction band, from extended valence states to tail states in the conduction band, as well as from tail states in the valence band to tail states in the conduction band, should be analyzed within the energy intervals corresponding to optical absorption values satisfying the condition $\alpha < (10^3-10^4) \text{ cm}^{-1}$.

In the strong absorption region of Ge-As-Se and Ge-As-Se-S chalcogenide glassy semiconductors (i.e., the Tauc absorption region above the mobility edge), the experimental dependence of the absorption coefficient (α) on the photon energy ($h\nu$) (Fig. 4) was analyzed by fitting to power-law type functions. The objective of this analysis was to identify deviations from the Tauc relation and to determine the actual energy dependence of the density of states. The

⁵ M.I. Abd-Elrahman et al. //Optical and electrical properties of thermally evaporated $\text{Se}_{90}\text{Sb}_{10}$ thin film. /Materials Science and Engineering B, Vol. 232-235, 2018, pp. 8-14.

study of the optical properties of chalcogenide glasses reveals that, in the strong absorption region ($\alpha > 10^4 \text{ cm}^{-1}$), the Tauc relation $(\alpha h\nu) = A(h\nu - E_g)^n$ may exhibit different values of the exponent n (1/2, 2, 3/2 and 3).

$$y=a \cdot (x-b)^c \quad (1)$$

The results of the comparative mathematical fitting between the Belehradec functional dependence (1) and the experimental dependence (Fig. 4) show that, for the $\text{Ge}_4\text{As}_{14}\text{Se}_{80}\text{S}_2$ and $\text{Ge}_{33}\text{As}_{17}\text{Se}_{15}\text{S}_{35}$ chalcogenide glassy compositions, power exponents of the dependence $\alpha \cdot h\nu \sim A \cdot (h\nu - E_g)^{p+s+1}$ exhibit $n=1.59$ and $n= 1.37$, respectively. These values, within experimental error, are close to $n \sim 3/2$, which is typically attributed to the presence of direct forbidden optical transitions⁶. In contrast, for the $\text{Ge}_{10}\text{As}_{20}\text{Se}_{60}\text{S}_{10}$ and $\text{Ge}_{26}\text{As}_{18}\text{Se}_{26}\text{S}_{30}$ compositions, the mathematical fitting results yield power exponents of $n=1.9$ and $n=2.1$, respectively. These values are consistent with $n \sim 2$, confirming that, in these compositions, optical absorption predominantly occurs through indirect allowed transitions⁷.

Considering that in amorphous materials, including chalcogenide glasses with amorphous structures, the densities of extended conduction and valence states can be expressed as $g_c(E_c) = G_c(E - E_c)^s$ and $g_v(E_v) = G_v(E_v - E)^p$, the dependence shown in Fig. 4 can be generally written in the following form:

$$\alpha h\omega = C' (h\omega - E)^{p+s+1} \quad (2),$$

here, C' is a quantity characterizing the probability of optical

⁶ S.K. Mohamed. Structural, optical, and electrical characteristics of $\text{Ge}_{18}\text{Bi}_4\text{Se}_{78}$ chalcogenide glass for optoelectronic applications //S.K. Mohamed, M.M. Abd El-Raheem, M.M. Wakkad et al./ Memories - Materials, Devices, Circuits and Systems 6, -2023, 100085

⁷ Bin Ye. Influence of the Selenium content on thermo-mechanical and optical properties of Ge-Ga-Sb-S chalcogenide glasses //Bin Ye, Shixun Dai, Wang et al. / Infrared Physics Technology . Volume 77, - 2016, Pages 21-26

transitions and depends on the p_{cv} -matrix element. Studies⁸ have shown that when $s=p=1/2$, i.e., when the energy distribution of the density of states near the conduction and valence band edges is parabolic, then $g_c(E_c) = G_c(E - E_c)^{1/2}$ and $g_v(E_v) = G_v(E_v - E)^{1/2}$.

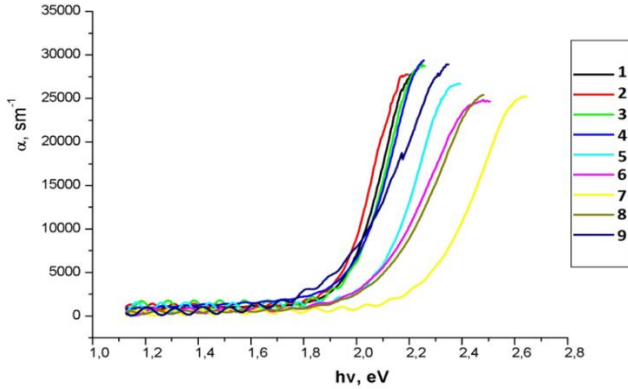


Fig.4. Dependence of the optical absorption coefficient (α) on the energy ($h\nu$) of the photon: 1 - $\text{Ge}_4\text{As}_{14}\text{Se}_{82}$, 2 - $\text{Ge}_4\text{As}_{14}\text{Se}_{80}\text{S}_2$, 3 - $\text{Ge}_7\text{As}_{16}\text{Se}_{72}\text{S}_5$, 4 - $\text{Ge}_{10}\text{As}_{20}\text{Se}_{60}\text{S}_{10}$, 5 - $\text{Ge}_{17.5}\text{As}_{15}\text{Se}_{52.5}\text{S}_{15}$, 6 - $\text{Ge}_{24}\text{As}_{19}\text{Se}_{37}\text{S}_{20}$, 7 - $\text{Ge}_{25}\text{As}_{10}\text{Se}_{40}\text{S}_{25}$, 8 - $\text{Ge}_{26}\text{As}_{18}\text{Se}_{26}\text{S}_{30}$, 9 - $\text{Ge}_{33}\text{As}_{17}\text{Se}_{15}\text{S}_{35}$

It should be noted that, considering the $N(E)dE \approx \rho^{d-1}d\rho$ relation for the density of extended states in a space of dimensionality d , and applying the proportional substitution into equation (2), for the parabolic distribution of the density of states near the conduction and valence band edges ($s=p=1/2$), one obtains $d=3$, which corresponds to a three-dimensional (3D) system. Experimental studies have shown that deviations from Tauc's relation are observed in both simple and multicomponent chalcogenide glasses. In other words, in various chalcogenide glasses, the reciprocal of the Tauc power exponent in the relation $[(\alpha \cdot h\nu)^{1/n} \sim f(h\nu)]$, may take values different from the ideal $m =$

⁸ Jai Singh. Advances in Amorphous Semiconductors /Jai Singh and Koichi Shimakawa // London, Taylor Francis , -2003, p.324

0.5. It has been established that the aforementioned experimental facts are related to the deviation of the density of states dependence on energy from that of free electron states. Instead of a d-dimensional space, the concept of fractal space dimensions (D) has been introduced⁹. Taking into account the expression for the density of extended states (3) and applying the substitution $p+s+1=(D_v+D_c-2)/2$, equation (2) can be rewritten in the form of relation (4) through fractal dimensions:

$$N(E) dE \sim E^{(D-2)/2} dE \quad (3),$$

$$\alpha \cdot hv = C' (hv-E)^{\frac{D_v+D_c-2}{2}} \quad (4)$$

Considering the expression $n=(D_v+D_c-2)/2$, the fractal dimensions (D) characteristic of the studied glassy materials were calculated, and the obtained results are presented in Table 2.

It follows that in $\text{Ge}_{10}\text{As}_{20}\text{Se}_{60}\text{S}_{10}$ and $\text{Ge}_{26}\text{As}_{18}\text{Se}_{26}\text{S}_{30}$ chalcogenide glasses, since the exponent of dependence (2) is $n \sim 2$, the condition $p = s = 1/2$ and $d = 3$ must be satisfied. In other words, in the obtained systems, the energy dependence of the density of extended conduction and valence band states is parabolic, and the systems possess three-dimensional characteristics.

According to the chemically ordered network (CON) model, it is assumed that Ge-S bonds form first, followed by Ge-Se bonds, then heteropolar (As-S, As-Se) bonds, and finally homopolar (Ge-Ge, As-As) bonds, in descending order of bond energy, thereby completing the formation of the matrix (Table 3).

⁹ B.B. Mandelbrot. The Fractal Geometry of Nature.// B.B. Mandelbrot/ New York, Freeman, -1982

Table 2.
Results of experimental and mathematical reconciliation
obtained from the results of optical experiments.

	Compositions	Z	R	A	Eg _{fit}	n= p+s+1	D _v +D _c	m=1/n	D=(D _v +D _c)/2
1	Ge ₄ As ₁₄ Se ₈₂	2,22	2,83	497482	1,85	1,86	5,72	0,537	2,86
2	Ge ₄ As ₁₄ Se ₈₀ S ₂	2,22	2,83	339057	1,86	1,59	5,18	0,628	2,59
3	Ge ₇ As ₁₆ Se ₇₂ S ₅	2,3	2,03	620888	1,847	1,852	5,704	0,539	2,852
4	Ge ₁₀ As ₂₀ Se ₆₀ S ₁₀	2,4	1,4	511748	1,826	1,9	5,8	0,556	2,9
5	Ge _{17,5} As ₁₅ Se _{52,5} S ₁₅	2,5	1,17	474963	1,834	2,54	7,08	0,393	3,54
6	Ge ₂₄ As ₁₉ Se ₃₇ S ₂₀	2,67	0,75	199965	1,786	2,35	6,7	0,425	3,35
7	Ge ₂₅ As ₁₀ Se ₄₀ S ₂₅	2,6	1	286200	1,879	2,587	7,175	0,315	3,587
8	Ge ₂₆ As ₁₈ Se ₂₆ S ₃₀	2,7	0,71	229019	1,845	2,1	6,2	0,476	3,1
9	Ge ₃₃ As ₁₇ Se ₁₅ S ₃₅	2,83	0,55	171075	1,828	1,37	4,74	0,729	2,37

A comparative analysis of the results presented in Tables 2 and 3 reveals that, in the compositions where the total relative fraction of tetrahedral structural units (GeS_{4/2}, GeSe_{4/2}), which satisfy the requirements of the chemically ordered network (CON) model and play a crucial role in the formation of the glassy matrix, exceeds the relative fraction of pyramidal structural units (AsSe_{3/2}) — namely, (Ge_{0.175}As_{0.15}Se_{0.525}S_{0.15}, Ge_{0.24}As_{0.19}Se_{0.37}S_{0.20}, Ge_{0.25}As_{0.10}Se_{0.40}S_{0.25}, Ge_{0.26}As_{0.18}Se_{0.26}S_{0.30}) — the fractal dimensions (D = 3.54; 3.35; 3.587; 3.1) are higher. This result is confirmed by the fact that in the studied compositions, the values of the number of constraints (N_{co}) and the mean bond energy (<E>) are higher, indicating the presence of strong topological network rigidity and chemical connectivity.

Table 3

Application of the chemically ordered network (CON) model to the investigated samples.

1. $\text{Ge}_{0.04}\text{As}_{0.14}\text{Se}_{0.82} = [2(\text{Ge}_{0.02}\text{Se}_{0.04})] \cdot [7(\text{As}_{0.02}\text{Se}_{0.03})] \cdot [53\text{Se}]$
2. $\text{Ge}_{0.04}\text{As}_{0.14}\text{Se}_{0.80}\text{S}_{0.02} = [0.5(\text{Ge}_{0.02}\text{S}_{0.04})] \cdot [1.5(\text{Ge}_{0.02}\text{Se}_{0.04})] \cdot [7(\text{As}_{0.02}\text{Se}_{0.03})] \cdot [53\text{Se}]$
3. $\text{Ge}_{0.07}\text{As}_{0.16}\text{Se}_{0.72}\text{S}_{0.05} = [1.25(\text{Ge}_{0.02}\text{S}_{0.04})] \cdot [2.25(\text{Ge}_{0.02}\text{Se}_{0.04})] \cdot [8(\text{As}_{0.02}\text{Se}_{0.03})] \cdot [31\text{Se}]$
4. $\text{Ge}_{0.10}\text{As}_{0.20}\text{Se}_{0.60}\text{S}_{0.10} = [2.5(\text{Ge}_{0.02}\text{S}_{0.04})] \cdot [2.5(\text{Ge}_{0.02}\text{Se}_{0.04})] \cdot [10(\text{As}_{0.02}\text{Se}_{0.03})] \cdot [10\text{Se}]$
5. $\text{Ge}_{0.175}\text{As}_{0.15}\text{Se}_{0.525}\text{S}_{0.15} = [3.75(\text{Ge}_{0.02}\text{S}_{0.04})] \cdot [5(\text{Ge}_{0.02}\text{Se}_{0.04})] \cdot [7.5(\text{As}_{0.02}\text{Se}_{0.03})] \cdot [10\text{Se}]$
6. $\text{Ge}_{0.24}\text{As}_{0.19}\text{Se}_{0.37}\text{S}_{0.20} = [5(\text{Ge}_{0.02}\text{S}_{0.04})] \cdot [7(\text{Ge}_{0.02}\text{Se}_{0.04})] \cdot [3(\text{As}_{0.02}\text{Se}_{0.03})] \cdot [13\text{Se}]$
7. $\text{Ge}_{0.25}\text{As}_{0.10}\text{Se}_{0.40}\text{S}_{0.25} = [6.25(\text{Ge}_{0.02}\text{S}_{0.04})] \cdot [6.25(\text{Ge}_{0.02}\text{Se}_{0.04})] \cdot [5(\text{As}_{0.02}\text{Se}_{0.03})]$
8. $\text{Ge}_{0.26}\text{As}_{0.18}\text{Se}_{0.26}\text{S}_{0.30} = [7.5(\text{Ge}_{0.02}\text{S}_{0.04})] \cdot [5.5(\text{Ge}_{0.02}\text{Se}_{0.04})] \cdot [1.33(\text{As}_{0.02}\text{Se}_{0.03})] \cdot [15.33\text{As}]$
9. $\text{Ge}_{0.33}\text{As}_{0.17}\text{Se}_{0.15}\text{S}_{0.35} = [8.75(\text{Ge}_{0.02}\text{S}_{0.04})] \cdot [3.75(\text{Ge}_{0.02}\text{Se}_{0.04})] \cdot [8\text{Ge}] \cdot [17\text{As}]$

In the $\text{Ge}_{0.33}\text{As}_{0.17}\text{Se}_{0.15}\text{S}_{0.35}$ chalcogenide glass composition, however, a deviation from the above-mentioned result is observed (Table 2). Considering the fractal dimensions (D) within the Porod dependence exponent formula $n_p = 6 - D$, it is revealed that n_p varies within the range $1 < n_p < 3$. This indicates that when n_p lies in the interval $1 < n_p < 3$, scattering centers with rough surfaces transform into volume-dimensional fractals. In contrast, for the samples with fractal dimensions $D = 2.37; 2.852; 2.86; 2.9$ (Table 2), the values of n_p vary within the range $3 < n_p < 4$, which demonstrates that in the corresponding compositions, the scattering centers are D-dimensional fractals with rough surfaces.

Thus, in the $\text{Ge}_{0.33}\text{As}_{0.17}\text{Se}_{0.15}\text{S}_{0.35}$ composition, consisting of

tetrahedral structural units (GeS_{4/2}, GeSe_{4/2}) and residual Ge and As atoms, the further reduction of fractal dimensions (D = 2.37) is associated with the formation of one-dimensional ethane-like structural units [(CH)Ge–Ge(CH)] within the three-dimensional glassy network.

To verify the accuracy of the mathematical fitting results, the dependence $(\alpha \cdot hv)^{1/2} \sim f(hv)$ corresponding to strong absorption ($\alpha > 10^4 \text{ cm}^{-1}$), based on the Tauc relation, as well as the dependence $(\alpha \cdot hv)^{2/3} \sim f(hv)$ associated with direct forbidden optical transitions, were constructed.

Table 4
Results demonstrating the agreement and minor deviations
between mathematical fitting and experimental findings.

Compositions	Z	R	A	Eg _{fit}	Eg1 Taus (1/2)	Eg2 Taus (2/3)	n=p+s+1	m=1/n
Ge ₄ As ₁₄ Se ₈₂	2,22	2,83	497482	1,85	1,856	1,9	1,46	0,6849
Ge ₄ As ₁₄ Se ₈₀ S ₂	2,22	2,83	339057	1,86	1,84	1,89	1,55	0,6451
Ge ₇ As ₁₆ Se ₇₂ S ₅	2,3	2,03	620888	1,847	1,86	1,92	2	0,5
Ge ₁₀ As ₂₀ Se ₆₀ S ₁₀	2,4	1,4	511748	1,826	1,85	1,92	1,94	0,5154
Ge _{17,5} As ₁₅ Se _{52,5} S ₁₅	2,5	1,17	474963	1,834	1,95	2,02	1,5	0,6667
Ge ₂₄ As ₁₉ Se ₃₇ S ₂₀	2,67	0,75	199965	1,786	1,88	1,98	1,44	0,6944
Ge ₂₅ As ₁₀ Se ₄₀ S ₂₅	2,6	1	286200	1,879	2,09	2,18	1,47	0,6802
Ge ₂₆ As ₁₈ Se ₂₆ S ₃₀	2,7	0,71	229019	1,845	1,91	2	1,63	0,6134
Ge ₃₃ As ₁₇ Se ₁₅ S ₃₅	2,83	0,55	171075	1,828	1,73	1,83	1,67	0,5988

By extrapolating to the value $\alpha=0$, the widths of the mobility gap (E_{g1e} }, E_{g2e}) (i.e., the optical band gap width) were determined, and the obtained results are presented in Table 4.

As seen from Table 4, the difference between the values of the mobility gap width (E_{gf}) obtained from mathematical fitting and the experimental values (E_{g1e} , E_{g2e}), unlike in the traditional approach, makes it possible to obtain more accurate information about the type of optical absorption transitions and, in particular, about the energetic distribution of the density of states at the edges of the valence and conduction bands [$g_c(E_c) = G_c(E-E_c)^s$ and $g_v(E_v) = G_v(E_v-E)^p$]. On the other hand, from Figure 5 it can be concluded that, as a result of the mathematical fitting between the Belehradec functional dependence (1) and the experimental dependence (Figure 4), the difference between the values of E_{gf} determined from the dependence $(\alpha \cdot hv)^{1/n} \sim f(hv)$ with exponent values $n=2$ and 1.94, and the values of E_{g1e} obtained from the experimental dependence $(\alpha \cdot hv)^{1/2} \sim f(hv)$, is negligibly small.

In contrast, the difference between the values of E_{gf} determined from the dependence $(\alpha \cdot hv)^{1/n} \sim f(hv)$ with exponent values $n = 1.46, 1.55, 1.5, 1.44, 1.47, 1.63,$ and 1.67 , and the values of E_{g2e} obtained from the experimental dependence $(\alpha \cdot hv)^{2/3} \sim f(hv)$, is negligibly small.

In Chapter Three, the relationship between the local structure of Ge–As–Se–S chalcogenide glasses and their glass transition temperature (T_g) was investigated. Experiments were carried out using differential scanning calorimetry (DSC) at a heating rate of 25 K/min (Fig. 5), and the results were analyzed within the frameworks of the chemically ordered network (CON) model, topological constraint theory (TCT), and Tanaka’s layered structure model.

To determine the glass transition temperature, semi-empirical expressions were used taking into account the mean bond energy $\langle E \rangle$ and the average coordination number Z . The results show that T_g reaches its maximum value for compositions corresponding to the chemical threshold $R = 1$. For example, for $Ge_{25}As_{10}Se_{40}S_{25}$, $\langle E \rangle = 2.77\text{eV}$, $Z=2.6$, and $R = 1$, and the theoretical and experimental results coincide.

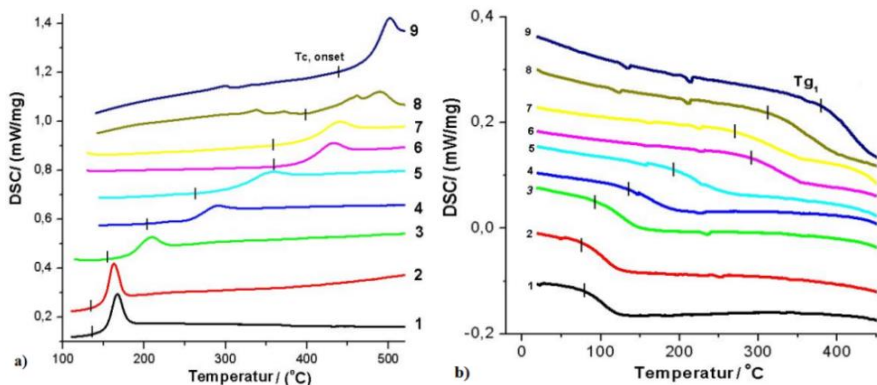


Fig. 5. Differential scanning calorimetry curves:
 1- $\text{Ge}_4\text{As}_{14}\text{Se}_{82}$; 2- $\text{Ge}_4\text{As}_{14}\text{Se}_{80}\text{S}_2$; 3- $\text{Ge}_7\text{As}_{16}\text{Se}_{72}\text{S}_5$;
 4- $\text{Ge}_{10}\text{As}_{20}\text{Se}_{60}\text{S}_{10}$; 5- $\text{Ge}_{17.5}\text{As}_{15}\text{Se}_{52.5}\text{S}_{15}$; 6- $\text{Ge}_{24}\text{As}_{19}\text{Se}_{37}\text{S}_{20}$;
 7- $\text{Ge}_{25}\text{As}_{10}\text{Se}_{40}\text{S}_{25}$; 8- $\text{Ge}_{26}\text{As}_{18}\text{Se}_{26}\text{S}_{30}$; 9- $\text{Ge}_{33}\text{As}_{17}\text{Se}_{15}\text{S}_{35}$.

The glass transition temperature calculated considering the mean bond energy shows good agreement with experimental values for certain compositions when $R \geq 1$. However, when $R < 1$, the difference between the experimental and calculated values of T_g increases.

The application of TCT shows that with an increase in the number of non-chalcogen atoms, the number of bond ($N\alpha$) and angular ($N\beta$) constraints increases, and the total number of constraints N_{co} rises with increasing Z . The condition $f = 0$ at $Z = 2.4$ corresponds to a rigid glassy state. However, $f = 0$ does not always yield the maximum T_g in these systems, since the theory does not account for the chemical nature of the bonds. Thus, TCT does not consider the character of chemical bonds or the average order of the local structure in chalcogenide glass compositions.

Tanaka's layered structure approach shows better agreement with experimental data, as it takes into account both chemical and topological order. In compositions with $f \approx 0$ and $R \approx 1$ ($\text{Ge}_{24}\text{As}_{19}\text{Se}_{37}\text{S}_{20}$, $\text{Ge}_{25}\text{As}_{10}\text{Se}_{40}\text{S}_{25}$, $\text{Ge}_{26}\text{As}_{18}\text{Se}_{26}\text{S}_{30}$, $\text{Ge}_{33}\text{As}_{17}\text{Se}_{15}\text{S}_{35}$), T_g and $\langle E \rangle$ reach high values, and the short- and medium-range order parameters also increase. $\text{Ge}_{25}\text{As}_{10}\text{Se}_{40}\text{S}_{25}$ was

selected as the most stable composition, with a difference between T_g and the crystallization temperature of $\Delta T_{c-g} = 87$ K. In this composition, as described by the CON model, tetrahedral $GeS_{4/2}$ and $GeSe_{4/2}$ units, as well as pyramidal $AsSe_{3/2}$ structural units, predominate, while homopolar bonds are absent.

The glass-forming ability (Hr) and thermal stability parameters also reach their highest values in compositions close to $R = 1$ and $f \approx 0$. For $Ge_{25}As_{10}Se_{40}S_{25}$, $Hr = 0.469$, $H' = 0.159$, and the index crystallation rapitidy (ICR) attains a minimum value. In contrast, in $Ge_{33}As_{17}Se_{15}S_{35}$, due to the decrease in Se and the increase in Ge and S, the concentration of tetrahedral structural units decreases, and the mean bond energy weakens, resulting in reduced Hr and stability, while the index crystallation rapitidy (ICR) increases. A high concentration of tetrahedral and pyramidal units strengthens the connectivity of the glassy network, which slows down the crystallization process. In such cases, the difference between T_g and T_c increases, enhancing the material's resistance to crystallization. Conversely, when residual homopolar bonds increase, crystallization becomes easier due to the effect of defects.

Thus, in Ge–As–Se–S glasses, optimal glass formation and high thermal stability are achieved under the conditions $R \approx 1$, $f \approx 0$, and $Z \approx 2.6$. In this case, the main structural units are $GeS_{4/2}$, $GeSe_{4/2}$, and $AsSe_{3/2}$, which explains both the high T_g and resistance to crystallization. Such compositions are considered promising materials for fiber-optic technologies.

In fiber-optic transmitters, a minimal index crystallation rapitidy coefficient is considered desirable for successful application. The index crystallation rapitidy (ICR) is calculated using expression (4) as the ratio of the crystallization peak height (MH) to its full width at half maximum (FWHM)¹⁰.

¹⁰ L. Saturday. Devitrification of Bi-and Ga-containing germanium-based chalcogenide glasses // L. Saturday, C. Johnson, A. Thai et al. //J. Alloys Compd., 674 (2016) 207–217

$$\text{ICR}=\ln(\text{MH}/\text{FWHM}) \quad (4)$$

One of the parameters characterizing the crystallization process is the fraction of crystallization at a given temperature, which is defined as the ratio of the area under the exothermic curve between the onset of crystallization and a specific T-temperature to the area of the corresponding crystallization peak at that temperature relative to the total peak area. The index crystallation rapitidy (ICR, on a logarithmic scale) undergoes significant changes within certain regularities depending on the modification. In all compositions where the relative concentration of tetrahedral ($\text{GeS}_{4/2}$, $\text{GeSe}_{4/2}$) and pyramidal ($\text{AsSe}_{3/2}$) structural units predominates, the crystallization rate coefficient is relatively low on a logarithmic scale. This result is explained by the increased connectivity of the amorphous matrix, including the mean bond energy ($\langle E \rangle$). The obtained results indicate that in samples close to topological rigidity conditions ($f \sim 0$; $\text{Nco} \sim 3$), index crystallation rapitidy (ICR) is relatively small, and the difference between the glass transition and crystallization temperatures ($\Delta T_{c-g} = 71\text{--}87 \text{ K}$) is large. In all compositions where the relative concentration of tetrahedral ($\text{GeS}_{4/2}$, $\text{GeSe}_{4/2}$) and pyramidal ($\text{AsSe}_{3/2}$) structural units predominates, the exponent (n) describing the temperature dependence of the crystallized volume fraction is relatively low within the intervals of $Z = 2.3\text{--}2.7$ and $R = 0.71\text{--}2.03$. Similarly, in compositions relatively close to topological and chemical ordering ($f \sim 0$; $\text{Nco} \sim 3$ and $R \sim 1$), the exponent (n) of the temperature dependence of the crystallized volume fraction exhibits two distinct minimal values ($n = 18.79$ and $n = 22.40$).

In the $\text{Ge}_{33}\text{As}_{17}\text{Se}_{15}\text{S}_{35}$ composition, with a high relative atomic fraction of Ge, index crystallation rapitidy and the exponent (n) of the temperature dependence of the crystallized volume fraction are relatively high ($\text{ICR} = -5.3$ and $n = 75.94$). This experimental result is explained by significant structure transformations observed in the local structure of the composition.

In Chapter Four, the objective is to determine the physical mechanisms and application potential of the sensitivity of complex-component Al–Ge₃₃As₁₇Se₁₅S₃₅–Te chalcogenide glassy semiconductor compositions with vacuum-deposited sandwich structures to a propane–butane gas mixture. To achieve this, the current–voltage characteristics (VAX) of the studied samples were measured on thin amorphous films with $d = 2 \text{ }\mu\text{m}$, deposited on glass substrates by vacuum thermal evaporation to form Al–Ge₃₃As₁₇Se₁₅S₃₅–Te sandwich structures.

The observation of transitions in the VAX from low-resistance to high-resistance states (or vice versa), i.e., current limitation at certain voltages along with partial oscillations in the dependence, is explained by the significant influence of U–centers with negative correlation energy on the generation–recombination processes, which play a decisive role in controlling charge transport in chalcogenide glassy materials (Fig. 6). Experimentally, increasing the gas concentration in the chamber leads to an increase in the sample’s resistance.

The working principle of sensors with resistance varying under gas exposure relies on the relative change in resistance depending on gas concentration, which is of particular practical importance.

This result indicates that Al–Ge₃₃As₁₇Se₁₅S₃₅–Te sandwich-structured samples based on chalcogenide glasses are highly sensitive to a propane–butane gas environment within the applied voltage range of $U = 0\text{--}10 \text{ V}$.

Additionally, the effect of a butane gas and benzene vapor environment on the VAX of the Al–Ge₃₃As₁₇Se₁₅S₃₅–Te sandwich structure was investigated, revealing that, compared to the open-chain structure of butane gas, the closed-chain structure of benzene vapor has a greater impact on increasing the resistance of the studied material. This result is associated with differences in the diameters and lengths of benzene and butane molecules, as well as the type, connectivity, and length of their bonds.

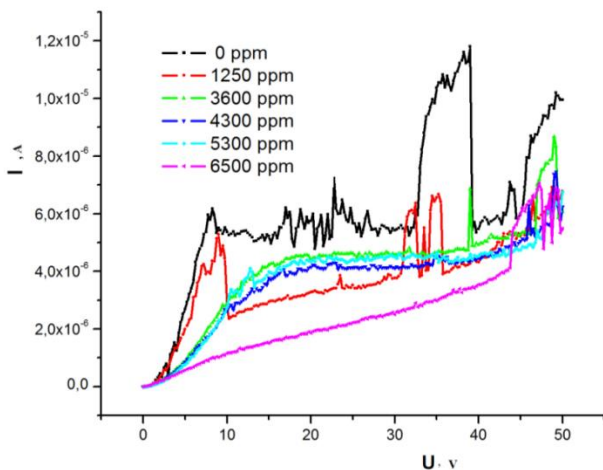


Fig. 6. Volt-ampere characteristic of the Al-Ge₃₃As₁₇Se₁₅S₃₅-Te sandwich structure in atmospheres containing air and a propane-butane gas mixture.

Thus, it was determined that the sample exhibits selective sensitivity depending on the type and concentration of the surrounding environment (Fig. 7).

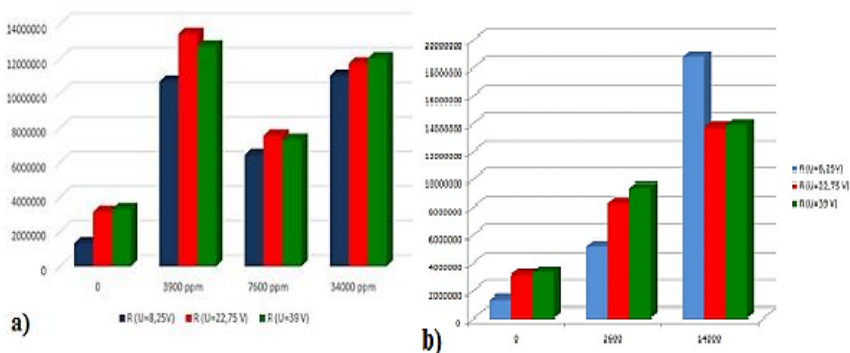


Fig. 7. Effect of butane (a) and benzene vapor (b) environments on the resistance of the chalcogenide glassy Ge₃₃As₁₇Se₁₅S₃₅ material

The volt-ampere characteristics of Al-Ge₃₃As₁₇Se₁₅S₃₅-Te sandwich structures in butane gas and benzene vapor environments were studied using the constant current method. It was shown that in both aliphatic and cyclic hydrocarbon environments, the current oscillations in the VAX gradually weaken and disappear. Compared to the open-chain structure of butane gas, the closed-chain structure of benzene vapor has a greater effect on increasing the resistance of the studied material, which is attributed to differences in the molecular diameters and lengths, as well as bond type, bond angle, connectivity, and bond length.

The gradual weakening and disappearance of oscillations is due to the accumulation of gas atoms in low atomic density regions or pores, which weakens the ionization processes of U⁻-centers and accelerates the periodic occupation of these centers by charge carriers.

It was found that in thin-film samples maintained in a butane gas environment within the experimental chamber, the accumulation of neutral gas atoms in low atomic density regions or pores causes a slight decrease in optical transparency in the near-infrared region of the spectrum, and a slight increase in optical transparency at wavelengths corresponding to the visible region ($\lambda \sim 597\text{--}600\text{ nm}$). These experimental results indicate that chalcogenide glasses have potential applications in fiber-optic gas sensors.

MAIN RESULTS

1. The local structure and glass transition processes of Ge–As–Se–S chalcogenide glassy materials were investigated using X-ray diffraction, differential scanning calorimetry, and analyzed within the frameworks of layered structure, topological constraint theory (TCT), and chemically ordered network (CON) models. It was shown that the $\text{Ge}_{25}\text{As}_{10}\text{Se}_{40}\text{S}_{25}$ composition is close to topological ($f \sim 0$) and chemical ordering ($R = 1$), exhibits crystallization resistance ($\Delta T_{c-g} \sim 87$ K), and has promising applications as a passive fiber-optic material.

2. It was determined that in materials close to topological rigidity conditions ($f \sim 0$; $N_{co} \sim 3$), the crystallization rate coefficient (ICR) is low, and the relatively high difference between glass transition and crystallization temperatures ($\Delta T_{c-g} = 71\text{--}87$ K) is associated with the high relative concentration of tetrahedral ($\text{GeS}_{4/2}$, $\text{GeSe}_{4/2}$) and pyramidal ($\text{AsSe}_{3/2}$) structural units forming the amorphous matrix.

3. In the $\text{Ge}_{33}\text{As}_{17}\text{Se}_{15}\text{S}_{35}$ composition with a high atomic fraction of Ge, the significant reduction in the glass–crystallization temperature difference ($\Delta T_{c-g} = 60$ K) and the increase in index crystallation rapidity (ICR) and exponent (n) characterizing the temperature dependence of the crystallized volume fraction are related to weak local structure transformations in the material.

4. It was shown that in the optical absorption spectra of Ge–As–Se–S chalcogenide glasses, deviations of the exponent in the Tauc dependence $[(\alpha \cdot hv)^{1/n} \sim f(hv)]$ from the ideal value $m = 1/n = 0.5$ are related to deviations of the energy dependence of the free electron state density from the parabolic form and are associated with the fractal nature of the studied materials.

5. According to the chemically ordered network (CON) model, it has been demonstrated that in those compositions where the overall relative fraction of tetrahedral structural units ($\text{GeS}_{4/2}$, $\text{GeSe}_{4/2}$), which play a crucial role in the formation of the glassy matrix, exceeds the relative fraction of pyramidal structural units ($\text{AsSe}_{3/2}$) ($\text{Ge}_{17.5}\text{As}_{15}\text{Se}_{52.5}\text{S}_{15}$, $\text{Ge}_{24}\text{As}_{19}\text{Se}_{37}\text{S}_{20}$, $\text{Ge}_{25}\text{As}_{10}\text{Se}_{40}\text{S}_{25}$,

Ge₂₆As₁₈Se₂₆S₃₀) — the larger values of fractal spatial dimensions ($D = 3.54; 3.35; 3.587; 3.1$) are associated with the higher values of the number of constraints (N_{co}) and the mean bond energy ($\langle E \rangle$).

6. It has been established that in Ge–As and Ge–S compositions, the characterization of the Porod dependence exponent (n_P) within the range $1 < n_P < 3$ provides evidence that scattering centers with rough surfaces transform into volume fractals.

7. The current–voltage characteristics of Al–Ge₃₃As₁₇S₃₅Se₁₅–Te sandwich structures in aliphatic and cyclic hydrocarbon environments were studied using the constant current method. It was shown that the accumulation of gas atoms in low-density regions or pores significantly affects the ionization and recombination processes of U^- –centers, sharply reducing current oscillations. This explains the selective sensitivity of the studied materials and their potential applicability in gas sensing.

DISSERTATION TOPIC PUBLICATIONS

1. Mehdiyeva S.İ., Ələkbərov R.İ., Məmmədov S.M., / Ge-As-Se-S xalkogenid şüşəvari sistemində rentgen difraksiya səpilməsi. // Azerbaijan Journal of Physics, -2021; XXVII, 4, s.7-10
2. Mehdiyeva S.İ., Ələkbərov R.İ., Məmmədov S.M. / Ge-As-Se-S xalkogenid şüşəvari maddələrində lokal quruluşun tədqiqi. / Akademik L.M. İmanovun 100 illik yubileyinə həsr olunmuş Molekulyar spektroskopiya mövzusunda konfrans Azərbaycan və rus dillərində məqalələr. -Bakı-Şuşa, - 21-22 Sentyabr, -2022, - s.125-127
3. Mehdiyeva S.İ., Ələkbərov R.İ., Məmmədov S.M. / Molekulyar quruluş modeli əsasında Ge-As-Se-S xalkogenid şüşəvari sistemində Raman səpilməsinin tədqiqi, H. Əliyevin 100 illiyinə həsr olunmuş nəzəri və tətbiqi fizikanın inkişafı mövzusunda beynəlxalq konfrans. Azerbaijan Journal of Physics. Section: C Conference H.A. Aliyev.-Bak; -08-09 June, -2023. -s.55-59
4. Alekberov R.I., Mekhtiyeva S.I., Mammadov S.M., /

- Peculiarities of topological phase transitions in Ge-As-Se and Ge-As-Se-S multicomponent chalcogenide glassy systems, Конференция; Аморфные и микрокристаллические полупроводники.- Санкт-Петербург, -3-5 июля 2023. -с.74-75.
5. Alekberov R.I., Mekhtiyeva S.I., Mammadov S.M. / Study of correlations between glass-transition temperature and local structure of Ge-As-Se, Ge-As-Se-S chalcogenide glasses. / Philosophical Magazine. Part A: Materials Science, -2023, 103(19), -p.1828-1841
 6. Mekhtiyeva S.I., Alekberov R.I, Mammadov S.M. / Study of local structure and thermal properties in fiber optics Ge-As-Se-S chalcogenide glass materials, International Conference on Advanced Laser Technologies (ALT). LS-I-10, -Samara, -September 18-21, -2023, -p.154.
 7. Alekberov R.I., Mekhtiyeva S.I., Mammadov S.M. / Glass transition, thermal stability and glass-forming tendency of Ge-As-Se-S glassy systems. / Journal of the Korean Physical Society, -2024;84: -p.694–702
 8. Mehdiyeva S.I. Propan-butan qaz qarışığına malik mühitdə Al-Ge₃₃As₁₇S₃₅Se₁₅-Te sendviç strukturunun volt–amper xarakteristikasının tədqiqi./ Mehdiyeva S.I., Ələkbərov R.I., Məmmədov S.M. [et al.] // Azerbaijan Journal of Physics, -2024; -2024, -s.23-27
 9. Mehdiyeva S.İ., Ələkbərov R.İ., Məmmədov S.M./ Ge-As-S-Se xalkogenid şüşəvari sistemində kristallaşma prosesinin tədqiqi. // Müasir təbiət və iqtisad elmlərinin aktual problemləri Beynəlxalq Elmi Konfrans, V hissə, -Gəncə, -3-4 may, -2024, -s.68-70
 10. Mehdiyeva S.İ., Ələkbərov R.İ., Məmmədov S.M. / Ge-As-S-Se xalkogenid şüşəvari sistemində kristallaşma prosesləri, Azərbaycan Milli Elmlər Akademiyasının xəbərləri, Fizika və Astronomiya, -2024; XLIV, 2, -s.17-23
 11. Mehdiyeva S.İ. Alifatik və tsiklik zəncir quruluşlarına malik karbohidrogen mühitinin Al-Ge₃₃As₁₇S₃₅Se₁₅-Te sendviç strukturunun volt–amper xarakteristikasına təsiri, / Mehdiyeva S.I., Ələkbərov R.I., Məmmədov S.M. [et al.] // Azerbaijan

- Journal of Physics. Section: C. Fizikanın aktual problemləri mövzusunda Beynəlxalq Elmi Konfrans / - Naxçıvan, 5-8 iyun, - 2024. –s.4-7
12. R Alekberov R.I., Mekhtiyeva S.I., Mammadov S.M. Glass-forming tendency in fiber optics Ge-As-Se-S chalcogenide glass materials, The 31th International Conference on Advanced Laser Technologies (ALT), -Vladivostok, -September 23-27, -2024, - p.134
 13. Alekberov R.I. Influence of hydrocarbon environment on electrical characteristics of Ge-As-Se-S chalcogenide glass system. / Alekberov R.I., Mekhtiyeva S.I., Mammadov S.M. [et al.] // Journal of advances in physics, -2024; 22, -p.249-255
 14. Alekberov R.I. The influence of a hydrocarbon environment with aliphatic and cyclic chain structures on the volt-ampere characteristic of the Al-Ge₃₃As₁₇S₃₅Se₁₅-Te sandwich structure, / Alekberov R.I., Mekhtiyeva S.I., Mammadov S.M. [et al.] // Chalcogenide Letters, vol. 21, N 11 (2024), pp 927-931
 15. Məmmədov S.M. Ge-As-Se-S xalkogenid şüşəvari sistemində optik udulmanın spektral asılılığının riyazi uzlaşdırma üsulu ilə tədqiqi, Azerbaijan Journal of Physics, -2025; XXXII; 3, -s.9-20



The defense will be held on 29 October at 09:30 the meeting of the Dissertation Council ED 1.14 of Supreme Attestation Commission under the President of the Republic of Azerbaijan operating at Institute of Physics Ministry of Science and Education Republic of Azerbaijan.

Address: AZ-1073, Baku, H.Javid ave., 131

Dissertation is accessible at the Library of Institute of Physics Ministry of Science and Education Republic of Azerbaijan.

Electronic versions of dissertation and its abstract are available on the official website of the Institute of Physics Ministry of Science and Education Republic of Azerbaijan.

Abstract was sent to the required addresses on 27
September 2025

Signed for print: 26.09.2025

Paper format: A5

Volume: 41870

Number of hard copies:20